A collimation system for ELI-NP Gamma Beam System – design and simulation of performance

G. Paternò [a,*], P. Cardarelli [a], M. Marziani [a,b], E. Bagli [a], F. Evangelisti [a,b], M. Andreotti [a,b], M. Gambaccini [a,b], V. Petrillo [c], I. Drebot [c], A. Bacci [c], C. Vaccarezza [d], L. Palumbo [e], A. Variola [d]

[a] *INFN – Sez. Ferrara, Via G. Saragat 1, I-44121 Ferrara, Italy*
[b] *Dipartimento di Fisica e Scienze della Terra, Università di Ferrara, Via G. Saragat 1, I-44121 Ferrara, Italy*
[c] *INFN – Sez. Milano, Via G. Celoria, 16 I-20133 Milano, Italy*
[d] *INFN – Laboratori Nazionali di Frascati, Via E. Fermi 40, I-00044 Frascati, Italy*
[e] *INFN – Sez. Roma, Università di Roma La Sapienza, Italy*

ARTICLE INFO

ABSTRACT

The purpose of this study was to evaluate the performance and refine the design of the collimation system for the gamma radiation source (GBS) currently being realised at ELI-NP facility. The gamma beam, produced by inverse Compton scattering, will provide a tunable average energy in the range between 0.2 and 20 MeV, an energy bandwidth 0.5% and a flux of about 10^8 photons/s. As a result of the inverse Compton interaction, the energy of the emitted radiation is related to the emission angle, it is maximum in the backscattering direction and decreases as the angle increase [1,2]. Therefore, the required energy bandwidth can be obtained only by developing a specific collimation system of the gamma beam, *i.e.* filtering out the radiation emitted at larger angles. The angular acceptance of the collimation for ELI-NP-GBS must be continuously adjustable in a range from about 700 to 60 µrad, to obtain the required parameters in the entire energy range. The solution identified is a stack of adjustable slits, arranged with a relative rotation around the beam axis to obtain an hole with an approximately circular shape. In this contribution, the final collimation design and its performance evaluated by carrying out a series of detailed Geant4 simulations both of the high-energy and the low-energy beamline are presented.

© 2017 Elsevier B.V. All rights reserved.

1. Introduction

ELI-NP is one of the three pillars of the ELI (Extreme Light Infrastructures) European Project, currently under realisation in Bucharest, Romania. This facility will host the Gamma Beam System (GBS), an intense and monochromatic gamma beam source based on Inverse Compton (IC) interaction between a high-power laser and an accelerated electron beam produced by a warm LINAC. The gamma beam is expected to feature an energy ranging from 0.2 to 20 MeV, a 0.5% energy bandwidth and a flux of about 10^8 photons/s. Such photon source will be devoted to the investigation of a broad range of applications, from nuclear physics and astrophysics, to material and life sciences.

The gamma beam generated by IC interactions is not intrinsically monochromatic and the photon energy is related to the emission angle [1,2]. In particular, the photons emitted along the electron beam axis feature the maximum energy, which in a first

approximation can be expressed by $E_\gamma \simeq \gamma_e^2 E_L$, where γ_e is the electron Lorentz factor and E_L the energy of laser photons, while the gamma photon energy decreases as the emission angle increases [3]. From the previous considerations it is apparent how the maximum energy of the gamma beam is tunable by adjusting the electron energy and that it is possible to select a desired energy band by properly collimating the gamma beam.

The EuroGammaS association, composed by many European research institutes and companies, lead by INFN, will provide the design, manufacturing, installation and commissioning of the GBS [4]. A fundamental part of GBS is represented by the characterisation and collimation line. The design of this system is shown in Fig. 1.

The collimation system is located inside a dedicated vacuum chamber (GCOLL) equipped with a system capable of controlling with high accuracy the alignment of the chamber in the tranversal directions, pitch and yaw. A concrete wall shields the characterisation line and the experimental areas downstream of the collimation from the secondary radiation due to the interaction of the primary gamma beams with the collimator. The characterisation
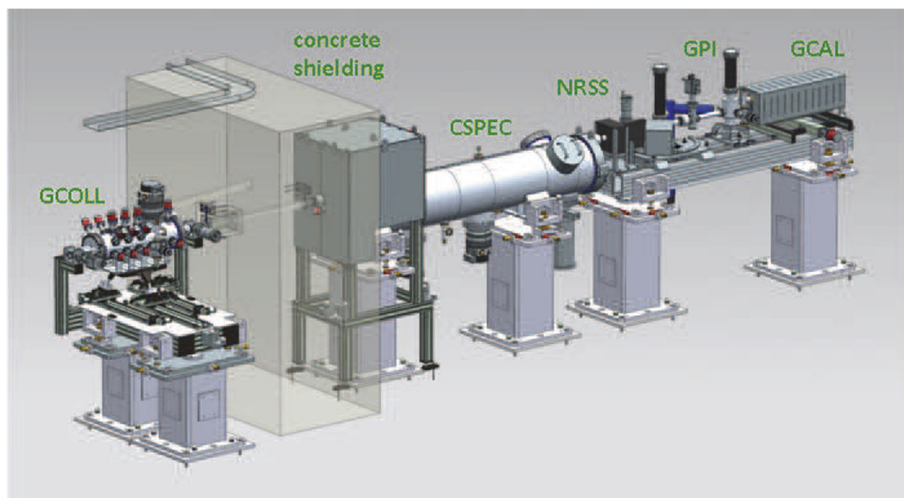
Fig. 1. Sketch of ELI-NP-GBS characterisation and collimation line.

of the collimated beam is performed through a Compton spectrometer (CSPEC) and an absorption calorimeter (GCAL), which measure the energy distribution and the photon yield respectively, a Gamma Profile Imager (GPI), which provides the photon spatial distribution, and a Nuclear Resonant Scattering System (NRSS) to calibrate the other instruments [5].

The collimation system is fundamental for the proper operation of the GBS, its main requirements are:

1. Continuously adjustable aperture, adaptable to the required maximum energy and bandwidth;
2. Effective attenuation of the gamma radiation;
3. Minimum contamination of the downstream experimental area with scattered radiation.

In order to cover the whole energy interval, the GBS will consist of two parallel beamlines with two separated interaction points (IPs) and collimation systems. The low energy line, for gamma energies ranging from 0.2 to 3.5 MeV, and the high energy line, which after a further acceleration of the electron beam, will allow to reach energies from 3.5 to 20 MeV. Two identical systems will be manufactured and delivered.

In this work, which represents an advance of the previous preliminary work [6], the optimal design identified for these collimation systems and a summary of the expected performance are described.

2. Materials and methods

In order to define the layout of the collimation system, a series of Monte Carlo simulations using MCNPX [7] and Geant4 [8] were carried out in the past few years to obtain a collimator configuration capable of satisfying the aforementioned requirements. The details of the final collimator design are shown in Fig. 2.

The collimator is composed of a stack along the beam axis of 14 slits with aperture independently adjustable (0–25 mm), mounted on a high precision stainless steel frame. The slits are divided in 3 groups of 4 slits, each with a relative rotation of 45° around the beam axis plus 2 additional slits positioned 20 cm apart from the previous ones to further clean the beam halo. The result is an hole with an approximately circular shape. Each slit is composed of 2 $40 \times 40 \times 20$ mm^3 blocks made of a 97% W alloy (2% Ni, 1% Fe) with a roughness smaller than 5 μm. This alloy provides similar attenuation of pure tungsten but has better mechanical properties.

The 2 blocks of each slit are mounted on a high precision linear guide. The motion is transmitted by two geared ball screws controlled by a stepping motor.

The optimal configuration and the performance of the designed collimation system has been evaluated in detail through a dedicated Geant4 application that simulates the transport of the gamma beam from the IP to the experimental area downstream the collimation system. As shown in Fig. 3, a complete geometry has been implemented in this new application. In addition to walls, floor, ceiling, shielding, vacuum pipe and other line relevant elements, it includes very accurate models of the collimation system and characterisation detectors.

The gamma beam used in our simulations is obtained by accelerating and transporting a realistic electron beam to the IP where its interaction with the laser beam occurs. The electron transport is simulated by using the TSTEP code, an updated version of PARMELA code [9], (from photocatode to photoinjector exit) and Elegant (from photoinjector to IP) [10]. A detailed description of this procedure can be found in Bacci et al. (2013) [11]. The simulation of the interaction between the electron beam and the laser pulse at the interaction point is performed by means of the Monte Carlo code CAIN [12]. This code generates a complete phase space of the gamma emission that is finally used as the source file for the simulation of the beamline and collimation system described in this work.

In particular, the simulation activities have been mainly focused on:

1. The evaluation of the energy bandwidth in relation to the collimation aperture;
2. The evaluation of the effect of possible misalignments on the energy bandwidth;
3. The analysis of the secondary radiation produced in the collimation process.

The simulations have been carried out for several gamma beam energies ranging from 0.2 to 19.5 MeV.

3. Results and discussion

The first part of the simulation process was carried out to finalize the design of the collimator as described above. In particular, the effect of using of a tungsten alloy with respect to pure W for the blocks of the slits was carefully evaluated, finding no apprecia-
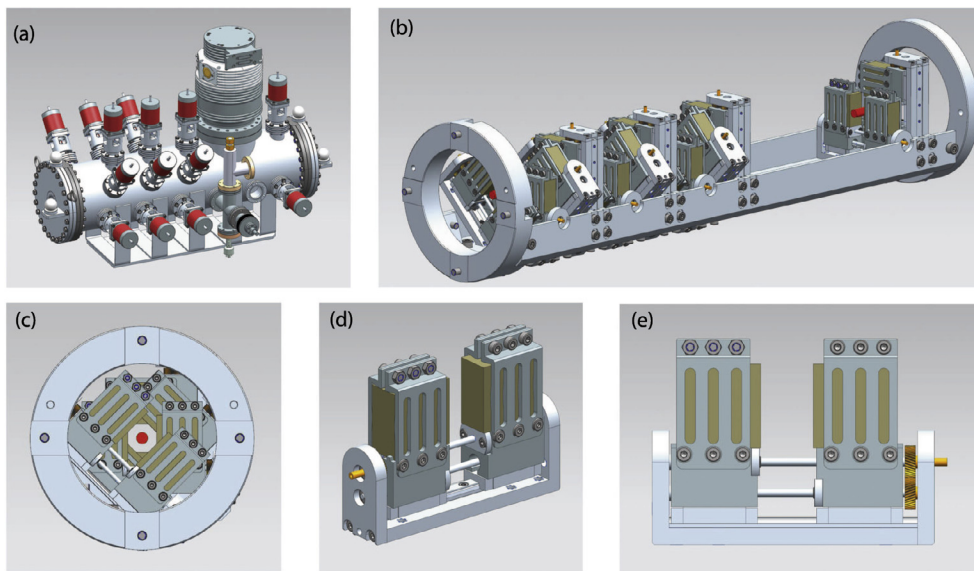
Fig. 2. Sketch of the collimation system. (a) Vacuum chamber containing the collimator. (b) Frame housing the 14 slits composing the collimator. (c) Collimation Hole. (d) Perspective view of a single slit. (e) Front view of a single slit.
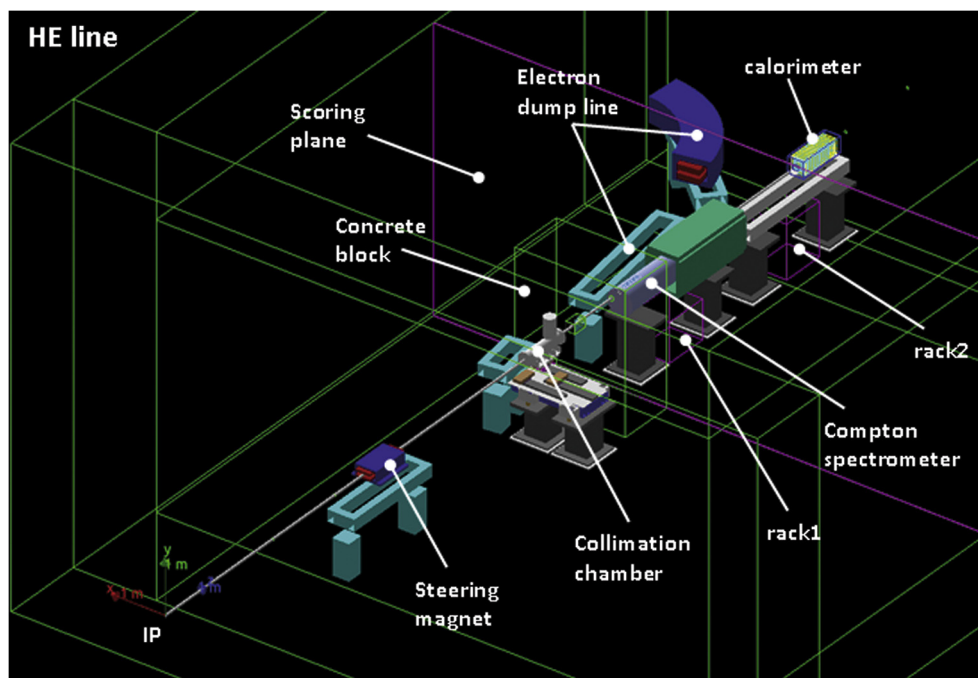

Fig. 3. Sketch of the high energy (HE) beamline of ELI-NP-GBS. This image was obtained directly from Geant4.

ble difference in the collimated beam and in the secondary radiation. Moreover, the choice of making 3 group of 4 slits with the same rotation around the beam axis was taken because from the simulation resulted that this configuration, together with the 2 additional slits position at the end of the stacks, guarantees less spurious events in the HPGe detector of the Compton spectrometer [4].

Given the above solution for the slits, the effect of the collimation on the final gamma beam energy distribution was evaluated, by studying the variation of the energy bandwidth (*RMS* value) as a function of the gap between the 2 blocks of each slits (aperture). In Fig. 4a are reported the simulation results concerning the energy distributions obtained at the scoring screen positioned just after the shielding wall (see Fig. 3) for the 10 MeV beam. In this case, an aperture of 3.0 mm leads to a relative bandwidth of 1.02%, corresponding to a beam divergence of 164 µrad and, as expected, the energy bandwidth decreases as the collimator aperture decreases. As a consequence, it is possible to see that the beam intensity is inversely proportional to the square of the aperture size. The same analysis was carried out for a wide range of gamma beams. Fig. 4b shows the collimator aperture required to obtain a 0.5% relative bandwidth as a function of the beam energy. As expected, this aperture decreases as the nominal energy of the beam increases because it is necessary to select a smaller and smaller portion of beam.
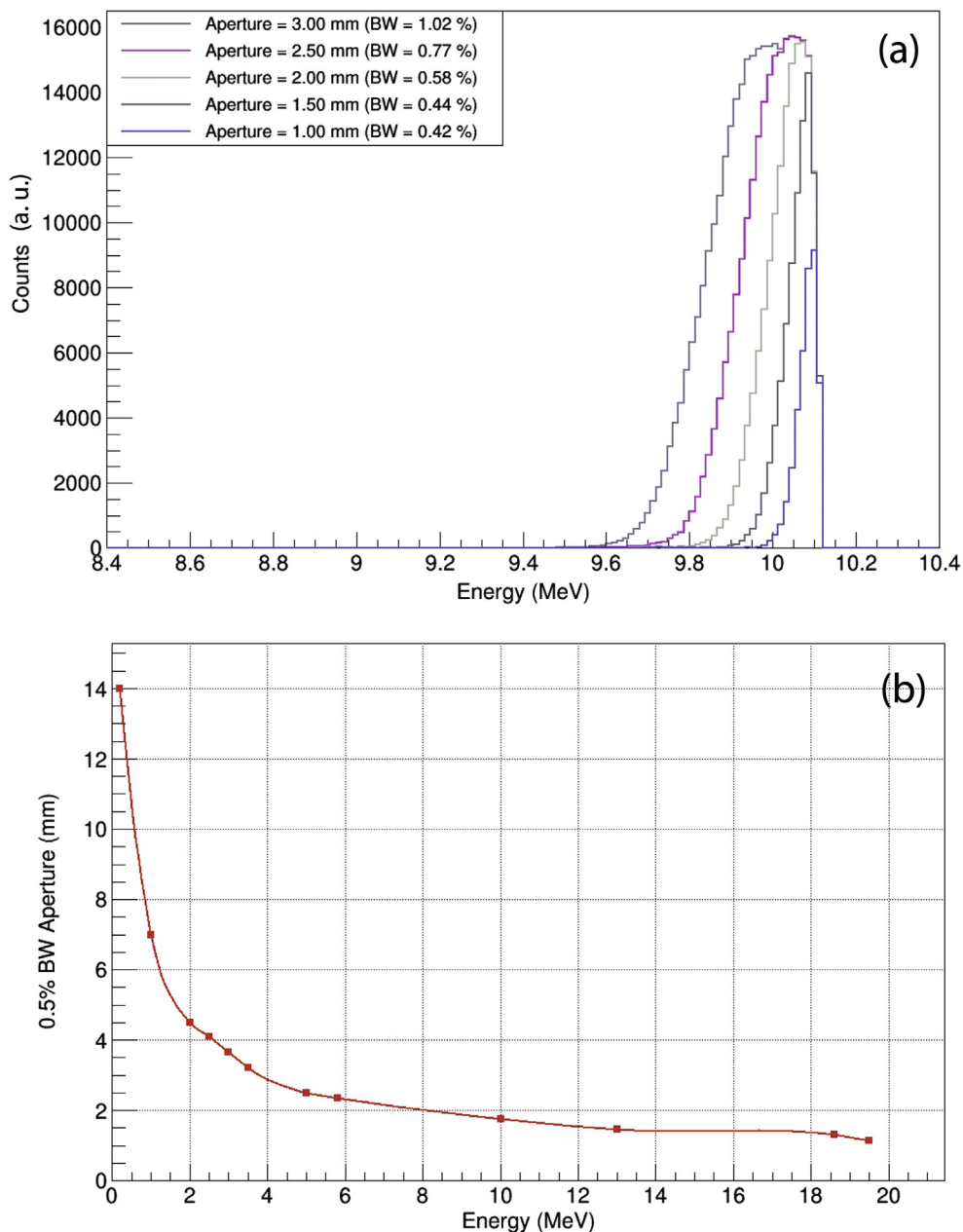
Fig. 4. (a) Energy distribution as a function of the collimator aperture for the 10 MeV beam. (b) Collimator aperture to obtain a 0.5% bandwidth as a function of the beam energy.

Another analysis concerned the study of the effect on the collimated beam of some non-idealities, such as the uncertainty on the aperture size of each slit, the misalignment of the blocks composing each slit with respect to the beam axis and the possible mispositioning and/or misalignment of the whole collimation chamber. A set of simulations were performed modelling each misalignment with a random variable with Gaussian distribution of increasing standard deviation σ. The three factors were considered alone and in combination. The most important factor resulted the misalignment of the slit blocks and it resulted to be more severe as the beam energy increases. Fig. 5 shows the effect of this misalignment on the collimated beam at 18.6 MeV. It causes a negligible decrease in the beam bandwidth and a decrease in beam intensity that reaches 20% for $\sigma = 100$ μm. However, the collimation system is expected to be assembled and aligned with a preci-

sion better of 50 μm and therefore the effect of this misalignment on the collimated gamma beam can be neglected.

The last analysis carried out concerned the background radiation in the proximity of the collimator, which can cause malfunctions of the gamma diagnostic detectors and their electronics of acquisition. This latter has to be placed as close as possible to the detectors to avoid delays in the acquired signals and therefore it will be housed in two racks placed under the Compton spectrometer (rack1) and the calorimeter (rack2), respectively. A set of simulations showed that the expected dose rate at the position of the racks is one or two orders of magnitude higher than the mean natural radiation background (see Table 1). This dose rate is due mainly to photons, in fact, no massive particles such as electrons, positrons or neutrons pass through the shielding wall for beam energy up to 5 MeV. At higher energies, racks receive a higher irradiation, mainly due to low-energy scattered photons and neutrons.
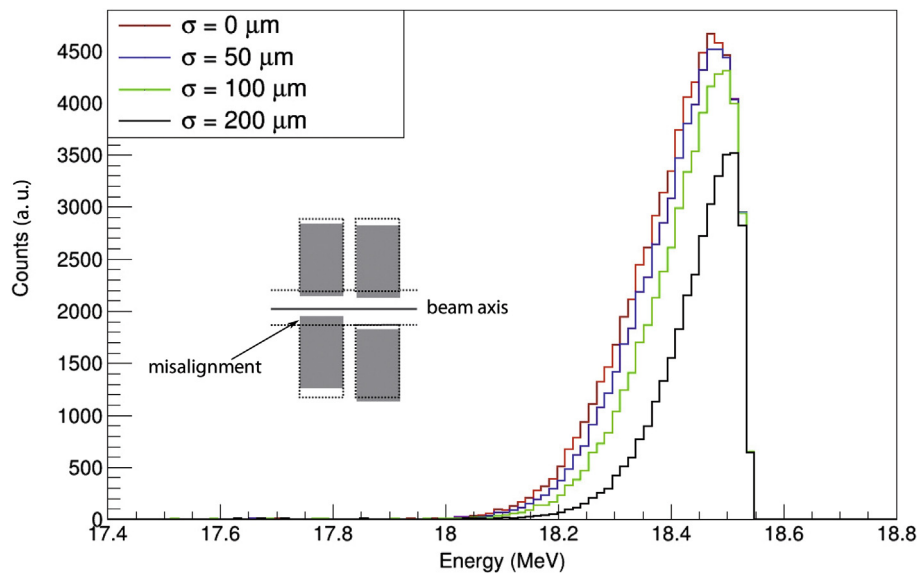
Fig. 5. Effect of slit misalignments for the 18.6 MeV beam. Each curve represents the gamma beam spectrum obtained with a different value of standard deviation of misalignment with respect to the beam axis.

Table 1
Dose rate in air at the position of the two data-acquisition racks for three beam energies.

Rack	E (MeV)	Dose-rate (Gy/s)
1	3	5.02×10^{-10}
1	10	7.99×10^{-10}
1	18.6	3.62×10^{-9}
2	3	2.52×10^{-10}
2	10	3.84×10^{-10}
2	18.6	3.41×10^{-9}

In general, the radiation level, is considered to be compatible with the intended operation of the gamma diagnostic detectors.

4. Conclusions

The final design and the performance analysis of the collimation system for both the low energy line and the high energy of ELI-NP-GBS was presented. The study was carried out through a detailed Monte Carlo simulation activity of the whole GBS. Results have shown that the required energy bandwidth (0.5%) can be attained using this system. The collimation aperture, and consequently the energy bandwidth, can be continuously adjusted to obtain the required value compatible with different applications. The effect of possible misalignments of the collimator on the gamma beam was investigated and it resulted to be compatible with the requirements. The secondary radiation along the vacuum pipe reaching the experimental area is negligible, when not absent. The background radiation in the area next to the collimation system, where a set of detectors for gamma diagnostic will be placed, was verified to be compatible with the operation of those devices.

References

[1] C. Vaccarezza et al., A European proposal for the compton gamma-ray source of ELI-NP, in: International Particle Accelerator Conference – IPAC'12, 2012, pp. 1086–1088.
[2] V. Petrillo et al., Photon flux and spectrum of gamma-rays compton sources, Nucl. Instrum. Methods Phys. Res. Sect. A 693 (2012) 109–116.
[3] C.A. Ur, Gamma beam system at ELI-NP, in: AIP Conference Proceedings, 1645, AIP Publishing, 2015, pp. 237–245.
[4] O. Adriani et al. Technical Design Report EuroGammaS proposal for the ELI-NP Gamma beam System. Published as arXiv:1407.3669 [physics.acc-ph], 2014.
[5] M.G. Pellegriti et al., Eurogammas gamma characterisation system for eli-np-gbs: the nuclear resonance scattering technique, Nucl. Instrum. Methods Phys. Res. Sect. A (2016).
[6] P. Cardarelli et al., Monte Carlo simulation of a collimation system for low-energy beamline of ELIGNP gamma beam system, Nucl. Instrum. Methods Phys. Res. Sect. B 355 (2015) 237–240.
[7] D.B. Pelowitz, MCNPX user's manual, Version 2.6.0. LA-CP-07-1473, Los Alamos National Laboratory, 2008.
[8] S. Agostinelli et al., Geant4 – a simulation toolkit, Nucl. Instrum. Methods Phys. Res. Sec. A 506 (3) (2003) 250–303.
[9] L. Young, J. Billen, The particle tracking code PARMELA, in: Proceedings of the Particle Accelerator Conference, 2003, p. 3521.
[10] M. Borland. Elegant: a flexible SDDS-compliant code for accelerator simulation, Aug 2000.
[11] A. Bacci et al., Electron linac design to drive bright compton back-scattering gamma-ray sources, J. Appl. Phys. 113 (19) (2013).
[12] K. Yokoya. User Manual of CAIN, version 2.40., http://lcdev.kek.jp/yokoya/CAIN/Cain242/CainMan242.pdf, 2009.